Predicting fire suppression in a simulated engine nacelle

J. C. Hewson
Fire Science and Technology
Sandia National Laboratories
Albuquerque, NM 87185-1135, USA

D. R. Keyser
INS, Inc.
PineHill Technology Park, Bldg. 1
48015-A Pine Hill Run Rd.
Lexington Park, MD 20653

Abstract

The Vulcan fire-field model is employed to simulate the evolution of pool fires and the distribution of fire suppressants in a engine nacelle simulator. The objective is to identify conditions for which suppression will and will not be successful in order to (1) provide input on experimental design and (2) to test the model's predictive capabilities through comparison with future test results.

Pool fires, where the fuel pool is on the bottom of the nacelle, have been selected for these tests because they have been identified as among the most challenging to suppress. Modeling of the production HFC-125 fire suppression system predicts that all pool fires are extinguished. Removing nozzles and reducing the rate of suppressant injection eventually lead to a predicted failure to suppress the fires. The stability of the fires, and therefore the difficulty in extinguishing them, depends on a variety of additional factors as discussed in the text.

1 Introduction

Suppression of fires in aircraft engine nacelles and other similar environments is challenging for a number of reasons. To begin with, these environments are highly cluttered. The clutter serves both to act as a flame stabilizer and to impede the transport of suppressant to this flame-stabilization region. High air-flow rates designed to remove combustible gases from the nacelle also act to rapidly remove suppressant from the nacelle, limiting the potential mixing time. Limits on the mass of suppression systems that can be carried while still allowing aircraft mission success are a further constraint. All of these physical realities contribute to a highly constrained set of requirements for successful fire suppression.

Previously, successful fire suppression systems have been developed through combined understanding of these issues and extensive testing. Detailed computational models, at the level of computational fluid dynamics (CFD), have shown limited success prior to this because of the complexity of the nacelle environment and the relatively high degree of accuracy required. However, new model developments and increased computational capabilities have moved CFD to a point where useful levels of prediction are now possible.

The physical device that is being computationally simulated is generally referred to as the "ground-based simulator," and this device is to be differentiated from computational simulations. Therefore, here we specify that further references to the "simulator" indicate the physical device located in the laboratory where experiments are performed while the "simulation" indicates the computational representation of the simulator.

2 Overall geometry

The engine nacelle simulations have been designed in accordance with measurements, drawings and visual inspections of the ground test simulator [1], located at Patuxent River Naval Air Station. The ground test simulator simulated here is a mock up of a port engine nacelle. Therefore, the port side corresponds to the outboard side of the engine, where air is introduced in flight, and the starboard side corresponds to the inboard side of the engine. The nacelle is roughly 3.18 m (125 in.) long.

The width and height vary significantly along the length, but are contained within a region 1.45 m high and 1.15 m wide. Coordinates are measured from a reference point on the top starboard side of the simulator test fixture so that all vertical coordinates are negative while other coordinates are positive. In conjunction with the rearward taper of the airframe, the nacelle is generally tallest and widest near the forward end, narrowing towards the aft. At various sections, there are larger cavities around the engine sides and top with additional space for air circulation. The lower nacelle surface slopes smoothly up from the forward to the aft, crossed by five ribs of varying heights. There are roughly four longerons running along the lower nacelle surface. The two central longerons end about 0.6 m before the aft end.

The engine, a hollow cylinder in the ground simulator, extends from the forward to the aft of the nacelle. The engine diameter is nominally 0.77 m with a slight narrowing over the front 0.61 m to a minimum diameter of 0.62 m. From 0.81 m aft to the aft end of the nacelle, the engine is uniformly 0.77 m in diameter. The outer surface of the engine is generally smooth, although various clutter items are attached to as will be described later.

In addition to the ribs and longerons, the most significant clutter is located near the forward end of the nacelle. It is dominated by a "gear-box" assembly located from 0.1 m to 0.75 m behind the forward end and primarily below the engine. The gear-box assembly is a collection of several parallelepiped and cylindrical objects of varying sizes that obstruct the flow in the large space between the engine and the lower nacelle in the vicinity of the air inlet scoop. Additional large parallelepiped clutter objects are located along the engine, particularly on the port side as far back as 1.5 m behind the forward end. Smaller clutter, primarily

tubing and wire bundles, exists along the lower half of the engine across the length of the nacelle. Some of this smaller clutter has been identified as a potential relight surface because of the relatively low thermal capacity and rapid heating to very high temperatures [2]. The afterburner control vanes at the aft end of the nacelle have not been included in the computational model because the setup (initially) focused on fire scenarios near the forward end of the nacelle.

3 Suppression model

Successful suppression by total flooding relies on providing a sufficient mass fraction of suppressant to all possible fire locations for a sufficient period of time. There are thus two key issues: First, supply a sufficient overall quantity of suppressant over time. Second, ensure that the suppressant is sufficiently distributed throughout the nacelle. The present section addresses the question of identifying what concentration of suppressant is sufficient while the subsequent sections address the suppressant distribution.

The Vulcan suppression model is described in detail in [3, 4] and only a summary will be given here. Suppression occurs when the fluid mixing time scales are short relative to the time required for combustion to occur. This can be quantified in terms of a critical Damköhler number where the Damköhler number is the ratio of the fluid mixing time to the chemical time. The fluid time scale used in the Vulcan suppression model is the Kolmogorov time scale, $\tau_\eta = 0.41(\nu/\epsilon)^{1/2}$ where ν is the fluid viscosity and ϵ is the rate of turbulent kinetic energy dissipation. The chemical time scale is determined using a perfectly-stirred reactor (PSR) model. A PSR has a characteristic mixing rate, the rate at which reactants are mixed into the reactor. Above a critical mixing rate, the rate of reactant mixing into the reactor exceeds the rate of reactant combustion and the flame "blows out." This critical mixing rate, τ_{chem}, in terms of the mass flux of reactant per mass of the reactor, defines the chemical time scale. Given τ_{chem} and τ_η, the flame is identified as extinguished if

$$\tau_{chem}/\tau_\eta > Da_{crit} \tag{1}$$

where $Da_{crit} = 0.563$ is obtained empirically by matching the blowout criteria for an ethane jet flame [5]. The chemical time scale is a function of the reactant enthalpy and concentrations, including that of the suppressant that increases the chemical time scale. Consequently, the value of τ_η at which the flame extinguishes increases corresponding with increases in the suppressant concentration as indicated in Fig. 1. A maximum fluid mixing time scale is imposed that corresponds roughly to a minimum mixing rate expected due to buoyant acceleration; such a limit is not captured at the subgrid scale in turbulence models.

4 Flow field

In the absence of fires and suppressant flow, the flow field in the nacelle is dominated by flow through an inlet air scoop located near the front of the nacelle coming up through the nacelle bottom. The inlet air flows from the inlet across the engine toward the upper aft of the nacelle. For the purposes of the simulations, an

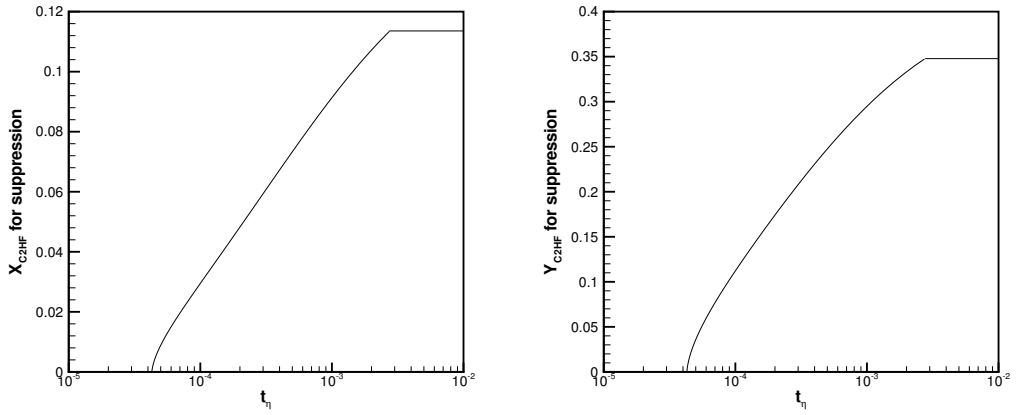

Figure 1: Suppressant mole (left) and mass (right) fractions required to extinguish flames for a given turbulent mixing time scale.

air mass flow rate of 1.0 kg/s has been considered.

The inlet air mass flow rates determine the air exchange times, the time over which the mass of air entering and leaving the nacelle equals the mass of air in the nacelle. For the simulation, the internal volume of the nacelle, neglecting clutter objects, is just over 1.4 m^3. This volume gives an air-exchange time of 1.6 s. The inlet cross section is approximately 0.008 m^2 and the inlet air flow velocity is approximately 150 m/s. This results in an inlet Reynolds number of 9×10^5 resulting in strong turbulence even without the clutter-enhanced mixing. The predominant predicted flow pattern is aftward flow along the bottom of the nacelle over the pool fires with forward flow along the upper portion of the nacelle.

4.1 Flow field with suppressant injection

The ground simulator was outfitted with a set of four suppressant nozzles that were found to be sufficient to suppress a fire when 3.2 kg (7 lbs.) of suppressant was discharged [2]. These are denoted by the numbers 1 through 4 with higher numbers corresponding to nozzles that are located toward the rear of the nacelle. Numerical simulations have been conducted for suppressant injection through these nozzles into the nacelle in the absence of a fire to obtain information on the distribution through the nacelle [1]. The suppressant was assumed to enter the nacelle in the vapor phase or to vaporize fast relative to other time scales. The suppressant mass flux for each nozzle was assumed to be proportional to the nozzle area.

The mass fraction of HFC-125 in vertical planes near the nacelle center and near the starboard and port sides are shown in Fig. 2 at the end of the 3 s suppressant injection period. In these contour plots the computational cells representing the nacelle, the engine and the clutter are blanked (white). The mass

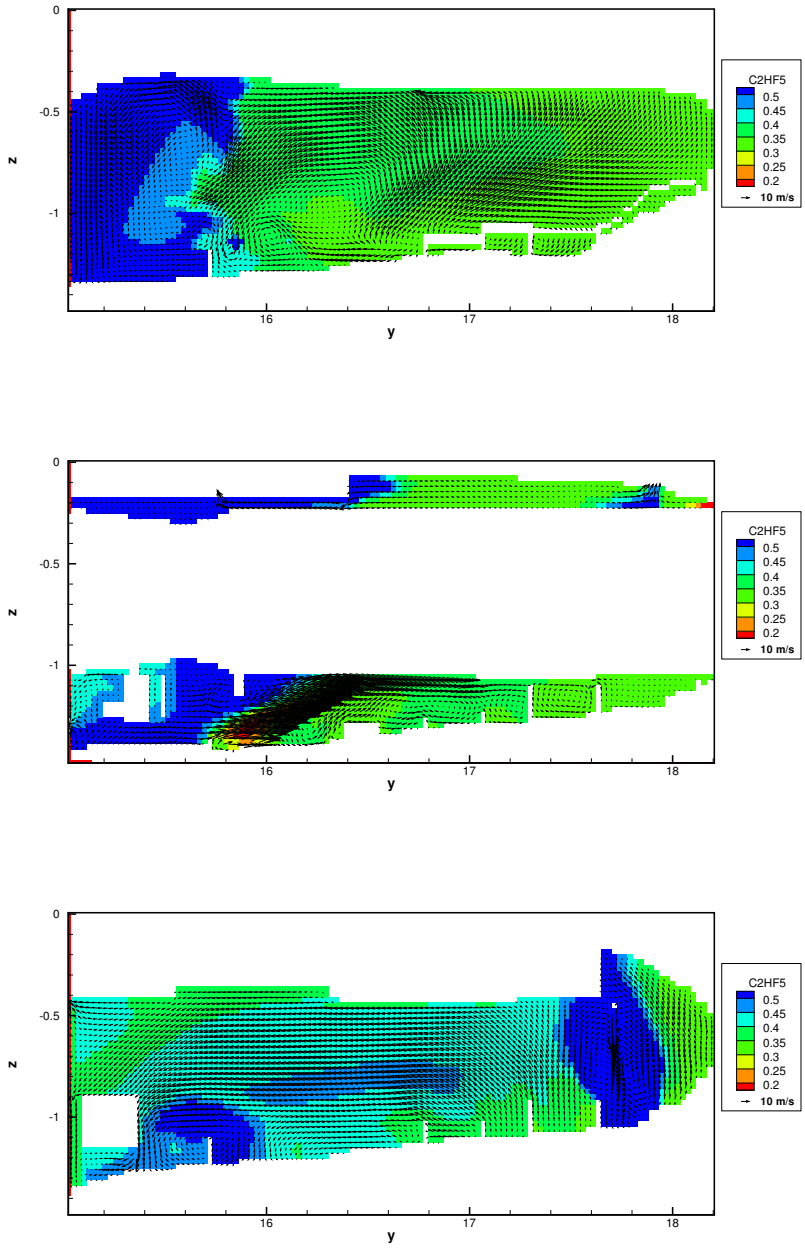

Figure 2: Contour plots of C_2HF_5 at 3.0 s after start of suppressant injection in vertical planes near the starboard side (top), near the nacelle centerline (center) and near the port side (bottom). Air flow into the nacelle is 1.0 kg/s; suppressant flow is 3.2 kg/s over 3 s.

fractions are colored in such a manner that blue and green (cool) colors indicate likely suppression and red (hot) colors indicate that suppression is unlikely. The critical mass fraction for suppression in the absence of intense mixing is somewhat less than 0.3 (closer to 0.25, so that this is a conservative estimate), and so the dividing line for likely suppression can be taken to be the dividing line between yellow-green and green. Depending on the turbulent mixing rates, suppression may occur for lower mass fractions of HFC-125. Velocity vectors are also provided in Fig. 2 to indicate the general flow direction.

Nozzle 1 is located on the starboard side of the nacelle in the forward section and is directed upward. The suppressant from nozzle 1 is observed to initially fill the upper forward nacelle and is advected into the lower forward nacelle. Nozzle 2 is located near nozzle 1 on the starboard side of the nacelle and directed to the port side across the top of the inlet air flow. Suppressant from nozzle 2 is dispersed aftward by the inlet jet along the nacelle. Nozzle 3 is located just past the mid-point of the nacelle, in between the second and third ribs, on the upper starboard side of the engine. Suppressant flow is directed at roughly a 45 degree angle upward across the engine and the majority of suppressant follows the mean flow forward along the upper nacelle. Nozzle 4 is located on the port side of the engine near the aft of the nacelle just behind the fifth rib. The suppressant is directed downward along the side of the engine in a direction that is counter to the general upward flow toward the upper diamond vent; this recirculation results in oscillations as the injecting gases are turned around to some degree by the mean flow.

5 Distribution of suppressant throughout the nacelle

As a measure of the sufficiency of suppressant distribution in the nacelle, the fraction of the nacelle volume for which the suppressant mass fraction exceed 30% has been used for characterization. Even with low intensity mixing, this amount is a generally sufficient level for suppression and represents a conservative estimate of suppression ability. Figure 3 shows this fraction when the air flow rate is 1.0 kg/s with varying rates of suppressant injection (same mass over different durations). The mass of suppressant to be injected was fixed at 3.2 kg and the period over which it was released varied from 2 to 6 s. Shorter injection periods would correspond to higher bottle pressures driving the injection process. To the extent that suppressant vaporization is slow, the period over which the suppressant is *effectively* injected will increase. Figure 3 shows that the entire volume is essentially filled for at least one second for injection durations of 3 s or less. For longer periods of injection, the volume is not filled with high concentrations ($> 30\%$) since suppressant is continually advected out the various vents. The failure to completely fill the nacelle does not indicate that suppression will not occur, but rather a less conservative regime where confidence in suppression is reduced.

The average peak suppressant mass fraction estimated [6] for the simulations shown in Fig. 3 are 0.59, 0.51, 0.44 and 0.35 with smaller mass fractions corresponding to the longer injection duration. If the turbulent mixing in the nacelle were sufficient to create homogeneity, the mass fraction throughout the nacelle would exceed 0.3 for all of these scenarios. Clearly, inhomogeneities arising from imperfect mixing are significant. This indicates that, while an analysis assuming complete homogeneity of the sort presented in [6]

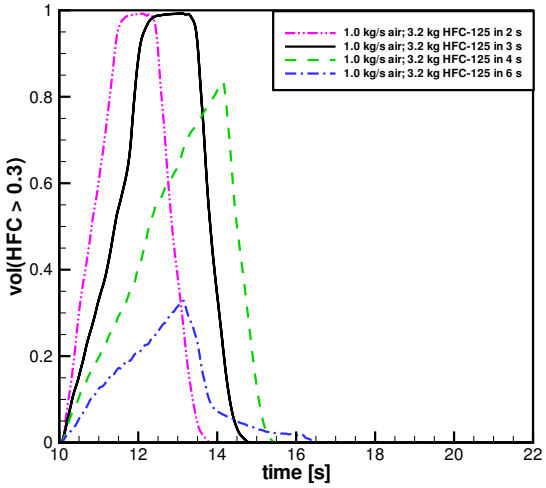

Figure 3: Fraction of the nacelle internal volume for which HFC-125 mass fractions exceeds 0.3 with 1.0 kg/s air flow into the nacelle. The mass of HFC-125 injected is 3.2 kg, injected over various periods as indicated with mass flow through each nozzle proportional to the measured nozzle-throat area.

does provide an indication of the trends, the CFD analysis can provide significant information on the degree of inhomogeneity. Specifically it can provide an estimate of the volume that fails to meet a criteria such as the one indicated here (suppressant mass fractions exceeding 0.3).

6 Influence of nozzles on suppressant distribution

A series of simulations has been conducted to ascertain the effect of removing a single suppressant nozzle while keeping the overall mass of suppressant injected constant. For this purpose, the total suppressant mass flow was also kept constant at 3.2 kg injected uniformly over 3 s. For these conditions, the nacelle volume fraction where the suppressant mass fraction exceeds 0.3 is evaluated. The results here are compared with those shown in Fig. 3 for all four nozzles functioning. In Fig. 3, the nacelle was completely filled, according to this criteria, for the range of flows considered.

In conducting simulations with specific nozzles removed, the mass flow rate out of the remaining nozzles was kept at the values used in other simulations. This corresponds to an assumption that the pressure driving the suppressant is not affected by the removal of a nozzle and that the nozzle cross sections have not been changed. The injection duration is thus increased to allow release of the full 3.2 kg of HFC-125.

The nacelle volume fraction where the suppressant mass fraction exceeds 0.3 is indicated in Fig. 4 with an air flow rate of 1.0 kg/s. In these and other scenarios [6], it appears that removing nozzle 3 has no detrimental effect since the complete volume is indicated as filled, and the duration for which it is filled is

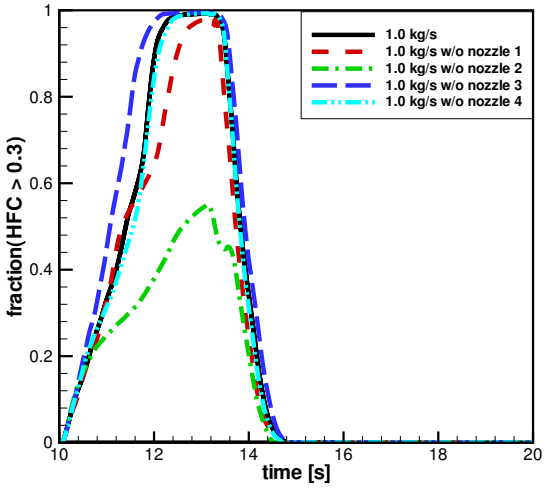

Figure 4: Fraction of the nacelle internal volume for which HFC-125 mass fractions exceeds 0.3 with all nozzles and with indicated nozzles blocked. The mass of HFC-125 injected is 3.2 kg, injected as described in the text. Air flow into the nacelle is 1.0 kg/s and suppressant mass flow through active nozzles is proportional to the measured nozzle-throat area.

increased because of the slightly slower rate of injection using three nozzles.

Based on the criteria shown in Fig. 4, removing nozzle 4 also has little apparent effect on the sufficient distribution of the suppressant. We note that the lower diamond vent in the nacelle simulator is modeled here as essentially blocked based on observations of the test simulator. Assuming that this vent is not blocked on fleet aircraft, the removal of suppressant in the aft region may be substantially faster making the retention of nozzle 4 highly desirable. Also, the additional vent in the aft region would mean that a greater portion of the suppressant injected through nozzle 4 would rapidly leave the nacelle. Additional simulations to consider the effect of an open diamond vent can help to address this question.

The removal of nozzles 1 or 2 does appear to have a significant effect on the distribution of suppressant throughout the nacelle. Suppressant from these nozzles is entrained in the air inflow; this entrainment by the air inflow significantly helps distribute suppressant throughout the nacelle [7]. The distribution of the suppressant mass fraction along the nacelle centerline is shown in Fig. 5 with nozzle 2 assumed to be capped; this can be be compared with Fig. 2. Nozzle 2 is located in the forward starboard area of the nacelle and directed across the lower nacelle in the port or outboard direction. Without nozzle 2 present, the inlet jet entrains relatively little suppressant and this results in little suppressant along the lower nacelle where pool fires might exist. It is clear that nozzle 2 plays a key role in distributing the suppressant throughout the nacelle through its interaction with the air inlet.

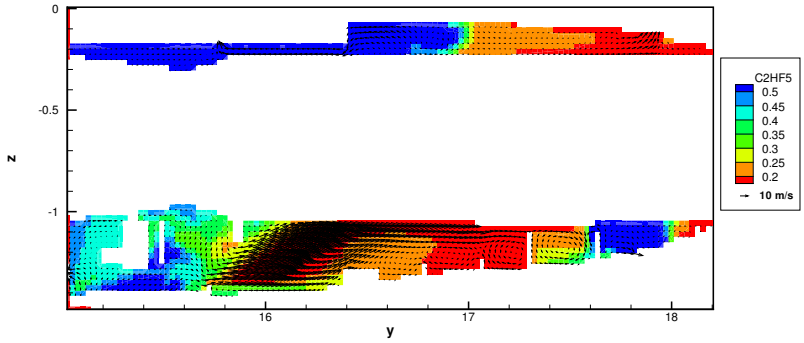

Figure 5: Contour plots of C_2HF_5 at 3.0 s after start of suppressant injection on the starboard side (top), near the nacelle centerline and on the port side (bottom). Nozzle 2 has been capped and suppressant flows through nozzles 1, 3 and 4 only. Air flow into the nacelle is 0.66 kg/s.

7 Pool Fires in the Nacelle

Pool fires stabilized behind obstructions have been identified as among the most challenging fires to suppress [8, 9]. Obstructions such as structural ribs provide a region of recirculating flow where hot products help stabilize the flame that suppressant is relatively slow to penetrate. In certain scenarios, such as those described in [4, 10, 11], the suppressant concentration must be maintained at an elevated level in the flow past the stabilization region for a substantial period of time to ensure that adequate suppressant penetrates the stabilization region.

Because the previous tests using the ground-test nacelle simulator focused on spray fires and since obstruction-stabilized pool fires are known to be challenging to suppress, the present study focuses on pool fire suppression. Pools located in four sections of the nacelle are considered. These sections are delineated from the forward to the aft end with increasing numbers as each rib is passed. The letter 'B' is applied as a prefix to the pool location to indicate that the pool is located between the two central longerons. These are the only locations where substantial quantities of fuel can collect. To augment the quantity of fuel, the basin just to the port of that indicated by 'B' is sometimes assumed to hold some fuel also; this basin is denoted with the prefix 'C.' The pool located at B1 is between the forward end of the nacelle and the first rib. That denoted B2 is located just aft of the first rib; the inlet air flows partially over this pool. The pool denoted B3 is located behind the second rib. The pool denoted B5C5 is located between the fourth and fifth ribs; these are the two larger ribs. The simulations indicate that pool fires at locations B4 and B6 are difficult to stabilize because of the particular predicted circulation. The approximate locations of the pools and the suppressant nozzles are shown in Fig. 6. The surface area of the largest possible pools in each section was measured in the ground-test simulator. Similar pool areas have been used in the simulations; the pool areas are indicated

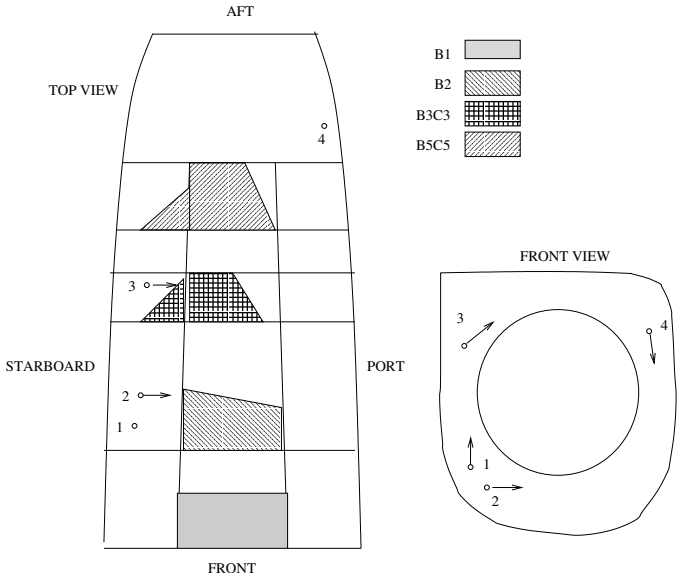

Figure 6: Schematic representation of the relative locations of the pool fires and the suppressant injection nozzles showing the ribs and central longerons. Not to scale.

Table I: Pool characteristics.

Pool	Area [m^2]	Pred. Evaporation rate [kg/s]	Volume of combustion	Volume where T > 700 K
B1	0.084	0.0089	5.9%	4.6%
B2	0.100	0.011	4.6%	22%
B3C3	0.094	0.0082	5.5%	37%
B5C5	0.043	0.0043	1.5%	5.2%

in Table I. The pools are assumed to be filled with JP-8, and the evaporation rate based on heat feedback to the pool is also indicated in Table I. In general, it is difficult to accurately predict the thermal feedback to a pool from a fire. Because these fires are partially advected beyond the pools by the convective flows in the nacelle, it is particularly hard to determine whether the evaporation rates are reasonable without suitable measurements. The evaporation rate is viewed as one of the significant uncertainties in the simulation (uncertainties may be as high as 50%). As a measure of the degree to which fires in different sections spread throughout the nacelle, Table I also shows the volume over which combustion is occurring and high temperatures exist. Heat release from pool fires B2 and B3C3 is substantially distributed throughout the nacelle by the main air inlet that passes over the fires in these regions.

8 Mixing times for clutter

There are two key challenges in suppressing clutter-stabilized pool fires. First, clutter creates a region in the recirculation zone where fluid mixing time scales may increase. As indicated in Fig. 1, this recirculation zone leads to an increase in the required suppressant. Second, there is a delay in the mixing of suppressant from the flow past the obstruction into the recirculation zone. This delay can be approximated using a perfectly-stirred reactor mixing model. Under such an assumption, the mean suppressant mass fraction in the flame stabilization zone, Y_{stab}, can be approximated as [12]

$$Y_{stab} = Y_{\infty}[1 - \exp(-t/\tau_{mix})] \tag{2}$$

where Y_{∞} is the mass fraction in the fluid flowing past the recirculation zone and τ_{mix} is the mixing time constant. For simple flow past a single step or rib with no other obstructions, Takahashi et al. [13] measured the mixing time constant to be

$$\tau_{mix} = 34.7(h/u^*) \tag{3}$$

where h is the obstruction height and u^* is the average of the mean velocity over the step and the mean velocity without the step. Based on the CFD simulation predicted velocities, it is possible to estimate mixing times using Eq. 3, although these estimates are complicated by the facts that the velocity varies laterally across the ribs and that the flow is not exactly normal to the ribs. For flow past the first rib, which stabilizes flames in pool B2, the mixing times range from very small where the inlet flow crosses the rib to 0.9 s where velocities are lower. For flow past the second rib, which stabilizes fires in pool B3C3, mixing times are in the vicinity of 0.1 to 0.2 s; mixing times for the third rib are similar. For flow past the large fourth and fifth ribs, which stabilize fires in pool B5C5, the mixing times range from 0.6 to 1.5 s. Except for the last set of ribs, the mixing times are generally small relative to the residence time for the suppressant in the nacelle so the finite mixing time is not expected to play a significant role.

Hewson et al. [4] showed that additional obstructions can affect the mixing time constant. In general, when obstruction wakes are coincident with the stabilization zone, the associated wake low-pressure region tends to pull the flow away from the stabilization zone and increase the time required for suppressant to mix into the flame stabilization zone. If the obstruction is located such that the high-pressure stagnation region in front of the obstruction is coincident with the stabilization zone, the opposite behavior is observed, resulting in reduced suppressant mixing times.

9 Suppression of pool fires

9.1 Results with four nozzle system

In this section, results of suppression simulations for various pool fires presented in Sec. 7 are reported using the four-nozzle configuration. In the following section, suppression predictions with individual nozzles

Table II: Fire suppression tests with an air flow rate of 1.0 kg/s.

Pool	Mass HFC-125 [kg]	Injection Rate [kg/s]	Active Nozzles	Suppression Time [s]
B1	3.2	1.07	1,2,3,4	0.8
B1	2.2	1.07	1,2,3,4	0.8
B2	3.2	1.07	1,2,3,4	0.9
B2	2.2	1.07	1,2,3,4	0.9
B3C3	3.2	1.07	1,2,3,4	1.2
B3C3	2.2	1.07	1,2,3,4	1.2
B3C3	3.2	0.53	1,2,3,4	none
B3C3	3.2	0.64	1,2,3,4	none
B3C3	3.2	0.71	1,2,3,4	none
B3C3	2.2	0.73	1,2,3,4	none
B5C5	3.2	1.07	1,2,3,4	1.8
B5C5	2.2	1.07	1,2,3,4	1.8

capped will be presented. In general, suppression is predicted for pool fires at all locations in the nacelle using the four-nozzle configuration with 3.2 kg of suppressant when this mass is injected over three or four seconds.

To examine the effect of varying the mass of suppressant injected and the rate of injection, a series of additional simulations for fires in pool B3C3 were conducted. When the rate of suppressant injection is reduced to just below 0.75 kg/s, no suppression was predicted in the simulations, although sustained burning would certainly be described as tenuous for these conditions since the fire was restricted to a corner of the pool C3. As the rate of suppressant injection is reduced, the fire stability increases, and at 0.53 kg/s the fire is clearly stabilized, at least near the corner of pool C3. The fire tends to stabilize in this location because the mixing rates are lower, as indicated in the following section. It is noteworthy that the mass of suppressant injected plays little role in determining the occurrence of suppression here. For the two cases with suppressant injection rates of 0.71 and 0.73, the resulting tenuous burning region is very similar. There will be a lower bound in terms of suppressant mass injected over a short period, although this has not been identified here. More significant in practice is the duration over which suppressant will act to inhibit reignition and allow cooling of heated surfaces. Thus the suppressant requirements are likely to be dictated by a combination of the rate required to flood the compartment with a high enough concentration and the mass required to maintain that concentration to inhibit potential reignition sources.

There is one complication that arises with high-boiling point agents, however. For high boiling point agents, the relevant parameter will not be the rate at which liquid suppressant is injected, but rather the rate at which the liquid suppressant vaporizes. The physics of the evaporation process are not captured in the present simulations but will be considered in subsequent simulations.

Though the detailed results are not presented here, suppression is sensitive to heat flux from the fire to the pool. If the heat flux and, hence, the fuel evaporation are reduced by 50%, suppression is substantially

easier for the cases considered in this section. For example, the reduced suppressant injection rates shown in Table II that fail to suppress the fire in pool B3C3 do succeed in suppressing the fire if the heat flux to the pool is reduced by 50%. The fire can be completely separated from the fuel source with slower evaporation rates. Similar results are expected if the fuel is cold or if there are substantial heat losses through the nacelle under the pool. While relatively high engine temperatures are expected during operations, temperatures during ground tests may be such that reduced evaporation is experienced.

9.2 Results with individual nozzles capped: inhomogeneities

In previous sections, the capping of various nozzles was shown to result in suppressant inhomogeneities that left certain regions with little suppressant as indicated in Fig. 4. Of significant interest was the flow over pools B2 and B3 when nozzles 1 or 2 were capped as indicated in Figs. 4 and 5. To examine the effects of these inhomogeneities on the predicted suppression, a series of simulations was conducted where one nozzle was assumed to remain capped. For the majority of these simulations, the flow rate out of the other individual nozzles was maintained at the flow rate that corresponds to 1.07 kg/s if *all* the nozzles were opened. This results in a reduced flow rate for the sum of the three remaining nozzles relative to the sum of the four nozzles and an increase injection duration. This case was evaluated to facilitate the experimental process since the bottle pressure remains fixed with and without nozzles capped with the per nozzle flow primarily related to the bottle pressure driving the flow. Results of these tests are summarized in Table III.

For fires in pools B1 and B5C5, the removal of various nozzles is not found to alter the prediction of suppression. For pool B1 the removal of either nozzle 1 or 2 has little effect beyond delaying the suppression for a short time. This delay in suppression appears to correspond to the overall slower suppressant injection since longer suppression times correspond to slower injection.

For pool B5C5, the removal of nozzle 2 results in an increase in the suppression time because suppressant from nozzle 2 is entrained in the air inflow and carried back across the ribs surrounding the pool. Without nozzle 2, the suppression is delayed until suppressant from other nozzles flows around the nacelle to be entrained by the air inflow. The removal of nozzle 4, which is closest to pool B5C5 and injects suppressant around the aft section of the nacelle, has minimal effect on suppression of this pool since the mean flow along the nacelle bottom is aftward.

For pool B3C3, the removal of nozzle 1 has little effect other than to slightly delay the suppression. Removing nozzle 2, however, results in a failure to suppress fires in pool B3C3. As indicated in Fig. 5, the removal of nozzle 2 leaves a significant volume with little suppressant. This volume is the volume directly over the pool B3C3, and thus nozzle 2 is necessary to suppress fires in this region.

For a pool located at B2, nozzle 1 is critical for suppression. Suppressant from nozzle 1 is entrained across pool B2 by the air inflow, and in the absence of that nozzle, the suppressant concentrations just over the pool are too low. Capping nozzle 2 also leaves a region deficient in suppressant shown in Fig. 5, but the air flow over this region (approaching 100 m/s) is sufficient to extinguish any fire in that region.

Table III: Fire suppression tests with an air flow rate of 1.0 kg/s and individual nozzles capped.

Pool	Mass HFC-125 [kg]	Injection Rate [kg/s]	Active Nozzles	Suppression Time [s]
B1	3.2	0.83	2,3,4	1.3
B1	2.2	0.83	2,3,4	1.3
B1	3.2	0.74	1,3,4	1.5
B1	2.2	0.74	1,3,4	1.5
B1	3.2	1.07	1,3,4	1.1
B1	3.2	1.07	1,3,4	1.1
B2	3.2	0.83	2,3,4	none
B2	2.2	0.83	2,3,4	none
B2	3.2	0.74	1,3,4	4.6
B2	2.2	0.74	1,3,4	3.2
B3C3	3.2	0.83	2,3,4	1.6
B3C3	2.2	0.83	2,3,4	1.6
B3C3	3.2	0.74	1,3,4	none
B3C3	2.2	0.74	1,3,4	none
B5C5	3.2	0.74	1,3,4	2.4
B5C5	3.2	0.90	1,2,3	1.7

10 Summary and Conclusions

Simulations of suppressant distribution and the suppression of pool fires in a simulated aircraft engine nacelle have been presented. Results indicate that the production suppression system, which injects roughly 3.2 kg of C_2HF_5 over a duration of 3 to 4 s, results in the distribution of suppressant over virtually all of the domain in concentrations sufficient to suppress a fire. As the rate of suppressant injection is reduced by a third or more, regions of the nacelle do not necessarily have sufficient suppressant for all fires. This is evidence of inhomogeneities in the concentration field since the estimated concentrations averaged over the nacelle are sufficient to suppress fires. Simulated fire suppression also fails as the rate of suppressant injection is reduced by a third or more. This observation has consequences for high-boiling point agents where the relevant rate of suppressant injection is the rate of liquid evaporation.

The removal of certain nozzles, specifically those denoted as nozzles 1 and 2, is predicted to result in substantial inhomogeneities in the suppressant distribution. Similarly, when fire suppression simulations are conducted with one of these nozzles capped, there is a predicted failure to suppress fires in certain regions. On the other hand, when the nozzle denoted as nozzle 3 is assumed to be capped, there is no apparent degradation is suppression capabilities. These results will need to be confirmed in subsequent tests.

Certain sensitivities have been identified in the present work and in the companion work [1] that will be further described in an upcoming report [6]. The pool vaporization rate, which is sensitive to fuel temperature, heat losses and details of the nacelle geometry, and the momentum associated with suppressant injection [1] have been identified as having particularly high sensitivities.

References

[1] Keyser, D. R., and Hewson, J. C., *Proceedings of the 2004 Halon Options Technical Working Conference*, (2004).

[2] Technical report, Northrop Grumman, El Segundo, California, (2000).

[3] Tieszen, S. R., and Black, A. R., *9th International Fire Science and Engineering Conference*, volume 1, Edinburgh, Scotland, (2004), INTERFLAM.

[4] Hewson, J. C., Tieszen, S. R., Sundberg, W. D., and Desjardin, P. E., *Proceedings of the Halon Options Technical Working Conference*, Albuquerque, NM, (2003).

[5] Tieszen, S. R., Stamps, D. W., and O'Hern, T. J., *Combust. Flame*, 106:442–446 (1996).

[6] Hewson, J. C., Technical report, Sandia National Laboratories, (2004) in preparation.

[7] Lopez, A. R., Gritzo, L. A., and Hassan, B., *Proceedings of the 1997 Halon Options Technical Working Conference*, Albuquerque, NM, (1997), , pp. 281–297.

[8] Hirst, R., Farenden, P. J., and Simmons, R. F., *Fire Technol.*, 12:266 (1976).

[9] Hirst, R., Farenden, P. J., and Simmons, R. F., *Fire Technol.*, 13:59 (1977).

[10] Takahashi, F., Schmoll, W. J., Strader, E. A., and Belovich, V. M., *Combust. Sci. Tech.*, 163:107–130 (2001).

[11] Hamins, A., andP. Borthwick, T. G. C., Gorchkov, N. N., McGrattan, K. B., Forney, G. P., Grosshandler, W. L., Presser, C., and Melton, L., in *Fire Suppression System Performance of Alternative Agents in Aircraft Engine and Dry Bay Laboratory Simulations* (R. G. Gann, Ed.), volume 2, NIST, 1995, pp. 1–199, .

[12] Hamins, A., Presser, C., and Melton, L., *Proc. Combust. Instit.*, volume 26, The Combustion Institute, Pittsburgh, 1996, pp. 1413–1420, .

[13] Takahashi, F., Schmoll, W. J., Strader, E. A., and Belovich, V. M., *Combust. Flame*, 122:105–116 (2001).